

SMAUG: A New Technique for the Deprojection of Galaxy Clusters

Fabio Pizzolato^{1,2}

¹ *Istituto di Fisica Cosmica, IASF/CNR, MILANO – Italy*

² *Dipartimento di Fisica, Università dell’Insubria, COMO – Italy*

This paper presents *SMAUG* (Spectral Modeling And Unfolding of Galaxy clusters), a new parametric technique for reconstructing the spatial distributions of hydrogen, temperature and metal abundance of the X-ray emitting gas of galaxy clusters. The spatial profiles of these quantities are described with analytical functions depending on few parameters. Since these profiles affect the shape of the emerging X-ray spectrum, the value of the parameters can be determined by fitting the model to the observed spectrum.

We describe the method and use it to work out the structure of the nearby cluster A1795. We combine the observation of the satellites *Chandra* for the core, *XMM-Newton* for the intermediate regions and *Beppo-SAX* for the outskirts. The relevant spatial distributions are derived directly from the spectra, thus allowing an immediate derivation of other indirect physical quantities like the gravitating mass, as well as a fast estimate of the profiles uncertainties.

1. Introduction

The intracluster medium (ICM) in galaxy clusters is a hot, rarefied and optically thin plasma in quasi-hydrostatic equilibrium within the cluster gravitational potential. The ICM emits radiation via thermal Bremsstrahlung and line emission, depending on its hydrogen density n_H , temperature T , and metal abundance Z .

Deducing the properties of the X-ray emitting gas in a cluster is complicated because the ICM is optically thin. The observed spectrum, projected against the sky, is actually an overlapping of 3-D spectra formed at different cluster depths, where the gas density, temperature and metallicity assume different values.

Of course the projection causes a loss of information, since the cluster actual 3-D structure is collapsed on its 2D projection on the sky. The reconstruction of the 3-D profile, therefore, calls for supplementary hypotheses on the distribution of the X-ray emitting gas, the most common being the spherical symmetry of the cluster.

There are various methods of deprojection: historically, the first were introduced by Fabian et al. (1981) and Kriss et al. (1983), and reconstructed the 3-D profiles starting from the cluster surface brightness. Other methods (Nulsen & Bohringer 1995; David et al. 2001; Allen et al. 2001; Buote 2000; Ettori 2002) exploit the spectral information as well; Ettori’s method, for instance, accumulates the spectrum of the cluster in concentric annuli centered on the X-ray surface brightness peak (see Figure 2), and analyses them to deduce the values of the projected quantities in each annulus. The outer rings subtend spatial regions progressively less affected by projection effects: an “onion peeling” process, i.e. an inwards recursive subtraction of their contribution to the inner rings yields the actual deprojected 3-D profiles. Often the resulting 3-D profiles are rather wiggly, and need to

be regularized before deriving other quantities like the shape of the gravitational potential.

2. SMAUG: A Parametric Approach to Deprojection

The methods previously sketched are essentially non-parametric. Here we present an alternative *parametric* approach (Pizzolato et al. 2003). *SMAUG* (Spectral Modeling And Unfolding of Galaxy clusters) is a new additive model we have implemented for the *XSPEC* X-ray analysis software package (Arnaud & Dorman 2000); it will be available to the community with the release 11.3 of the software.

The image of the cluster is accumulated in concentric rings centered about the X-ray emission peak. N_H , T and Z are given analytic expressions depending on the 3-D radius r , and some parameters a_1, \dots, a_N . These functions are flexible enough to encompass a wide range of qualitative behaviors of these profiles (for further details, see Pizzolato et al. 2003).

The observed spectral flux of photons emitted by the region of a cluster subtending a ring of projected radii b_1 and b_2 is

$$\mathcal{F}_E = \frac{4\pi}{D_A^2(1+z)^2} \int_{b_1}^{b_2} db b \int_b^\infty dr \frac{r}{\sqrt{r^2 - b^2}} \epsilon_{E(1+z)}(r),$$

where z is the redshift, D_A is the angular distance and $\epsilon_E = n_H^2(r) \Lambda_E [T(r), Z(r)] / E$

is the photon emissivity of the plasma. This double integral may be reduced to a single integral, making possible the calculation of a model spectrum:

$$\mathcal{F}_E = \frac{4\pi}{D_A^2(1+z)^2} \int_{b_1}^\infty dr K(r; b_1, b_2) \epsilon_{E(1+z)}(r)$$

$$K = \begin{cases} r \sqrt{r^2 - b_1^2} & \text{if } r < b_2 \\ r \left(\sqrt{r^2 - b_1^2} - \sqrt{r^2 - b_2^2} \right) & \text{if } b_2 < r \end{cases}$$

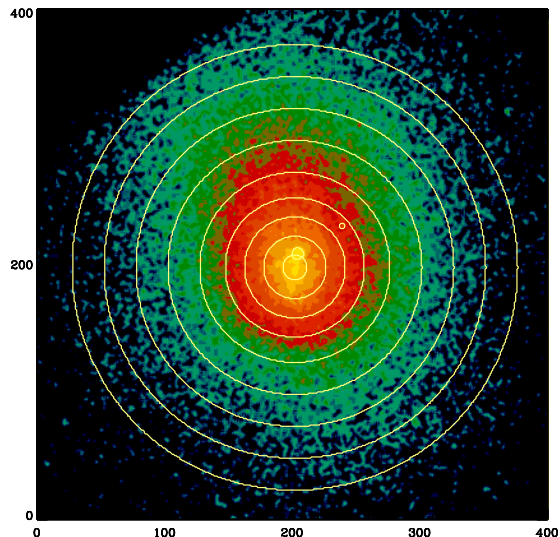


FIG. 1.— The deprojection rings overlapped to the X-ray image of A1795. (From Ettori et al. 2002).

SMAUG calculates the model $\mathcal{F}_E(a_1, \dots, a_N)$ for the observed spectrum, and (under *XSPEC*) this is simultaneously fit to the observed spectra of the rings. The best-fit values of the parameters a_1, \dots, a_N are determined iteratively. The statistical uncertainties of the fit parameters are used to estimate the errors of the deprojected profiles. From the newly determined functions $n_H(r)$, $T(r)$ and $Z(r)$ other quantities (like the pressure or the gravitational mass) are easily computed.

3. Example: The Deprojection of A1795

A1795 is a nearby ($z = 0.0631$) and relatively relaxed cluster. We have analyzed simultaneously the observations from 3 satellites covering a wide range of the cluster: from 10 kpc to 1.5 Mpc: *Chandra* for the 5 inner rings, *XMM-Newton* for the intermediate 4 rings and finally *Beppo-SAX* for the 4 outer rings. The spectra of these annuli are fitted simultaneously, in order to gain a good accuracy in the determination of the 3-D profiles. It has been necessary to take into account the cross-normalization uncertainties, i.e. the different responses of the instruments. The upper panels in Figure 2 show the analytically deprojected hydrogen density, temperature and metal abundance profiles. The curves are the best-fit profiles yielded by our analytical deprojection, and the boundaries correspond to a one-sigma error in the parameters. The markers show the data and error bars from the matrix geometrical deprojection method of Ettori (2002). Circles correspond to *Chandra* data, triangles to *XMM-Newton* and diamonds to *Beppo-SAX*. The lower panels in the same figure plot the ratio between the 3-D quantities derived from the geometrical and the analytical deprojection. Note that the temperature profile shows a sharp edge around 37 kpc. We consider positively the ability of our functional form of $T(r)$ to spot such an unexpected behavior.

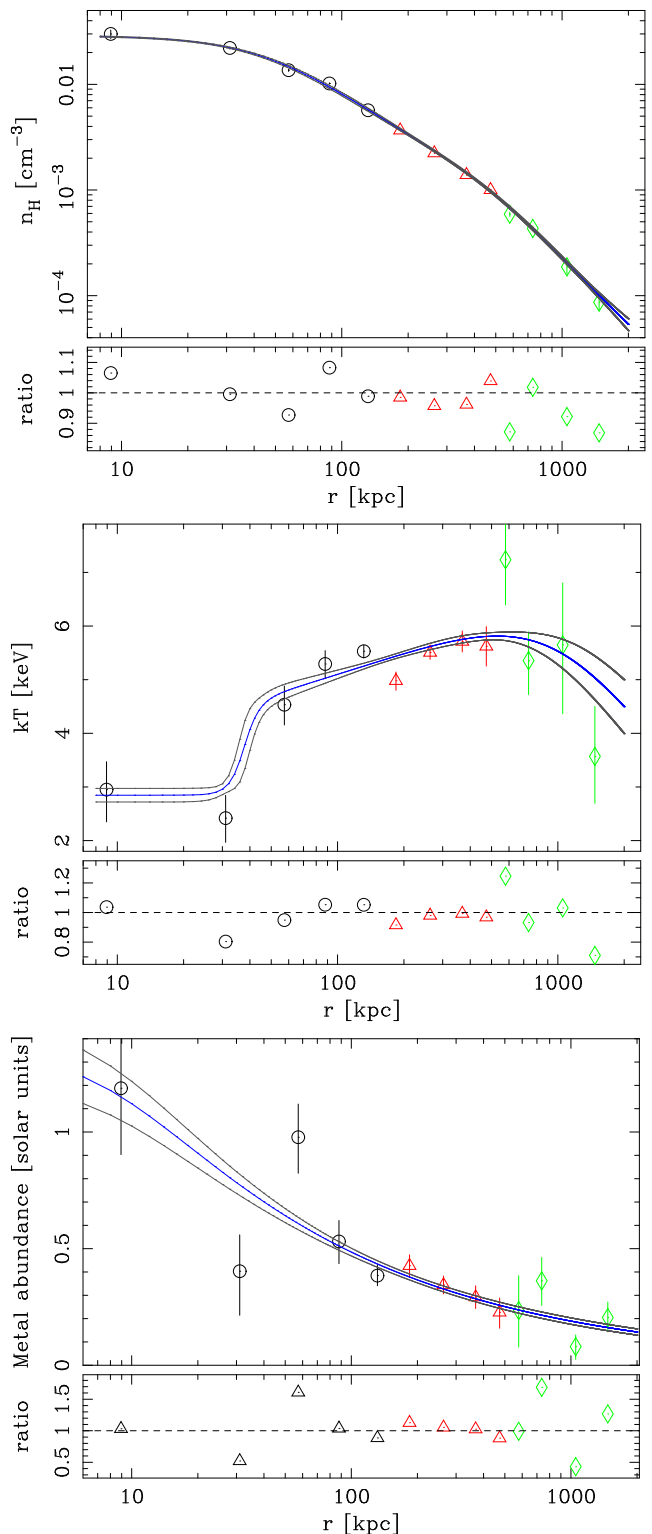


FIG. 2.— The hydrogen density, temperature and metal abundance profiles obtained with *SMAUG* and with Ettori's matrix deprojection technique. Circles correspond to *Chandra* data, triangles to *XMM-Newton* and diamonds to *Beppo-SAX*. Further details in the main text.

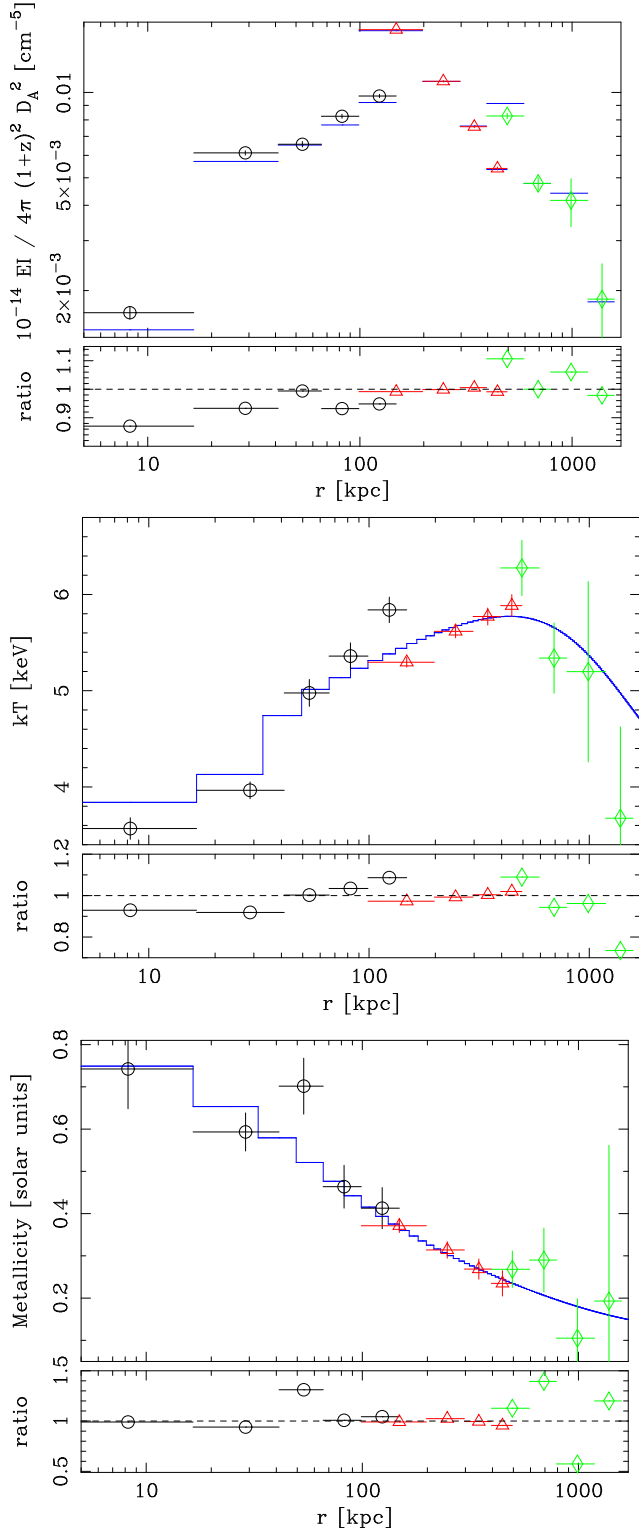


FIG. 3.— The re-projected quantities, compared with those directly observed. The symbols are the same as in Figure 2. More details in the main text.

3.1. Back to Flatland: Checking the Reliability of Our Results

A powerful check of the deprojected results is to take the 3-D reconstructed profiles of density, temperature

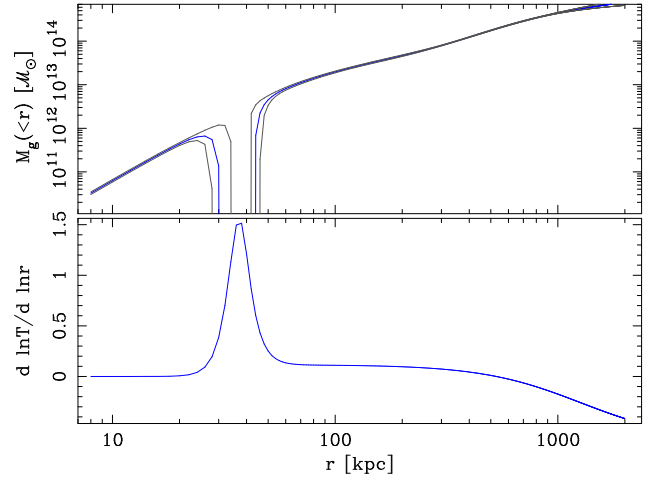


FIG. 4.— The profile of the gravitating mass within radius r (upper panel), and the slope of the temperature profile (lower panel). More details in the text.

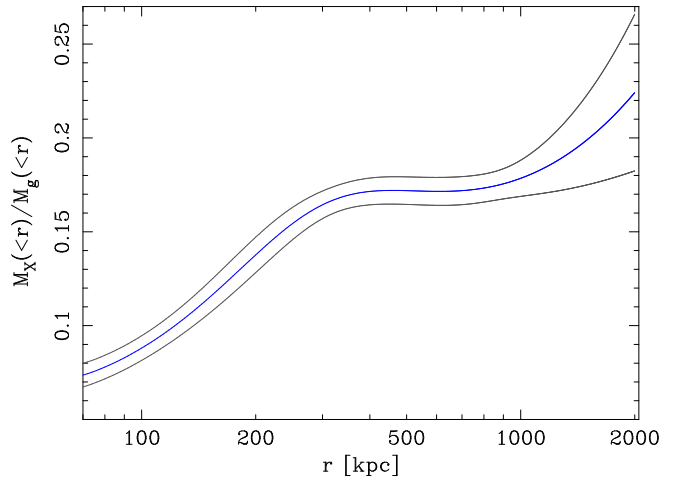


FIG. 5.— The fraction of the X-ray emitting mass.

and metal abundance, fold them again and compare to the observed ones. As shown in Figure 3, the agreement is good, showing that the analytical model fits the data adequately.

3.2. The Gravitating Mass, the Gas Fraction and the Iron Mass

The knowledge of the 3-D density, metal abundance and temperature profiles allows an easy determination of the profiles of other quantities.

The knowledge of the 3-D density and temperature profiles, together with condition of hydrostatic equilibrium, allows to determine the gravitating mass $M_g(<r)$ of A1795 (fig 4). The dip around 37 kpc is due to the edge in the temperature profile, which breaks down the hypothesis of hydrostatic equilibrium at that radius. The temperature edge is best appreciated in the lower panel, plotting the logarithmic derivative of the temperature profile. By integrating the 3-D gas density and calculating the gravitating mass, it is possible to reconstruct their ratio $M_X(<r)/M_g(<r)$, i.e. the fraction of X-ray

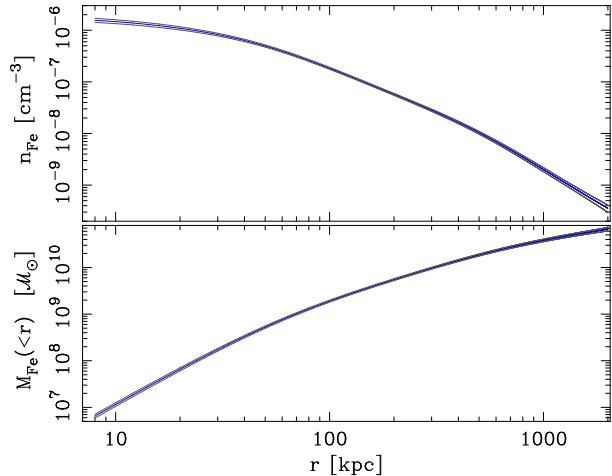


FIG. 6.— The iron density profile (upper panel) and the enclosed iron mass (lower panel).

emitting gas within radius r . This plot excludes the innermost region where the hydrostatic equilibrium fails. The slight rise in the outskirts is statistically significant only at the $1\text{-}\sigma$ level, and should not be taken too confidently.

Finally, from the 3-D metal abundance and the hydrogen density it is possible to recover the iron distribution across the cluster (Figure 6).

In all the plots the error curves correspond to $1\text{-}\sigma$ uncertainty in the parameters.

4. Summary

We have developed SMAUG, a new parametric method for the X-ray spectral deprojection of galaxy clusters. This model has been implemented as an *XSPEC* model, and will be available to the community starting from the 11.3 release of *XSPEC*. This technique differs with respect to other non-parametric techniques, in that it does not require any regularization of the 3-D profiles, but is as accurate. *SMAUG* works with explicitly known parametric fitting functions for $n_H(r)$, $T(r)$ and $Z(r)$. Therefore the spectral fitting procedure yields directly the values of the best-fit parameters, as well as their uncertainties. The use of known functional forms for the spatial profiles of n_H , T and Z allows a straightforward derivation of other indirect physical quantities.

I wish to thank Silvano Molendi, Sabrina De Grandi, Simona Ghizzardi, Stefano Ettori and Keith Arnaud.

References

- Allen, S. W., Ettori, S., & Fabian, A. C. 2001, *MNRAS*, 324, 877
 Arnaud, K. & Dorman, B. 2000, An X-Ray Spectral Fitting Package User's guide for version 11.0x, NASA/GSFC HEASARC Laboratory for High Energy Astrophysics, Greenbelt, MD
 Buote, D. A. 2000, *ApJ*, 539, 172
 David, L. P., Nulsen, P. E. J., McNamara, B. R., Forman, W., Jones, C., Ponman, T., Robertson, B., & Wise, M. 2001, *ApJ*, 557, 546
 Ettori, S. 2002, *MNRAS*, 330, 971
 Ettori, S., Fabian, A. C., Allen, S. W., & Johnstone, R. M. 2002, *MNRAS*, 331, 635
 Fabian, A. C., Hu, E. M., Cowie, L. L., & Grindlay, J. 1981, *ApJ*, 248, 47
 Kriss, G. A., Cioffi, D. F., & Canizares, C. R. 1983, *ApJ*, 272, 439
 Nulsen, P. E. J. & Bohringer, H. 1995, *MNRAS*, 274, 1093
 Pizzolato, F., Molendi, S., Ghizzardi, S., & De Grandi, S. 2003, *ApJ*, 592, 62